

## Cavitating Propeller

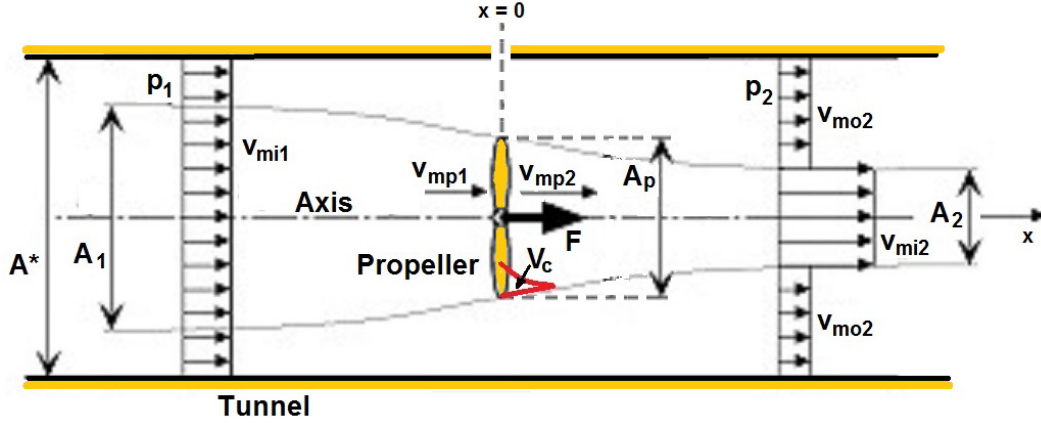


Figure 1: Schematic and notation of a propeller in a tunnel (the cavitation volume is shown in red).

In this section we construct and analyze the transfer function for a cavitating propeller in a water tunnel as depicted in Figure 1; this configuration allows for analyses of both an axial flow pump ( $A^*/A_p = 1$ ) and a propeller mounted in a water tunnel ( $A^*/A_p > 1$ ). The analysis is based on the unsteady, one-dimensional flow model developed in Section (Mfi) that, in turn, is related to the steady flow analysis in Section (Mfc). As with the other transfer functions presented, the methodology applies to linear perturbations and therefore the first step is to linearize all the equations (Mfi1)-(Mfi14) by dividing all the unknowns into the steady or mean flow part denoted by an overbar and the fluctuating part denoted by the tilde. Thus, for example, the upstream flow velocity is expressed as

$$v_{mi1} = \bar{v}_{mi1} + Re \{ \tilde{v}_{mi1} e^{j\omega t} \} \quad (\text{Nrs1})$$

where  $\omega$  is the fluctuation frequency. After substituting similar expressions for all the unknowns, equations (Mfi1)-(Mfi14) are then divided into steady and unsteady parts and linearized under the assumption of small fluctuations. The unsteady parts of the equations consist of a set of linear equations for the unsteady components, the eight unknowns  $v_{mo2}$ ,  $v_{mi2}$ ,  $v_{mp2}$ ,  $v_{mp1}$ ,  $A_1$ ,  $A_2$ ,  $F$ , and  $p_2$  as well as the quantities,  $v_{mi1}$ ,  $p_1$ ,  $\beta$  and  $dV_c/dt$ . The unsteady component of  $\beta$  is obtained by the linearized version of the equation for  $\beta$  in Section (Mfg), which diminishes for larger values of  $\sigma$ . The rate of change of cavity volume,  $dV_c/dt$ , is given by equation (Mfi15). Using these equations, we can construct the conventional transfer matrix (Brennen 1994) that relates the downstream fluctuations to the inlet fluctuations:

$$\begin{Bmatrix} \tilde{p}_2^T \\ \tilde{m}_2 \end{Bmatrix} = \begin{bmatrix} T_{11} & T_{12} \\ T_{21} & T_{22} \end{bmatrix} \begin{Bmatrix} \tilde{p}_1^T \\ \tilde{m}_1 \end{Bmatrix} \quad (\text{Nrs2})$$

where  $p^T$  and  $m$  are the total pressure and the mass flow rate, respectively.

Figure 2 presents a typical calculation of the transfer matrix for an advance ratio of  $J_1 = 1.0$  and duct cross-sectional areas of  $A^*/A_p = 1, 2$  and  $10$ . For illustrative purposes, values of the compliance and mass flow gain factor ( $K^*/2\pi$ ,  $M^*$ ) of  $(0.1, 1.0)$  were selected since these values are typical. The change of the

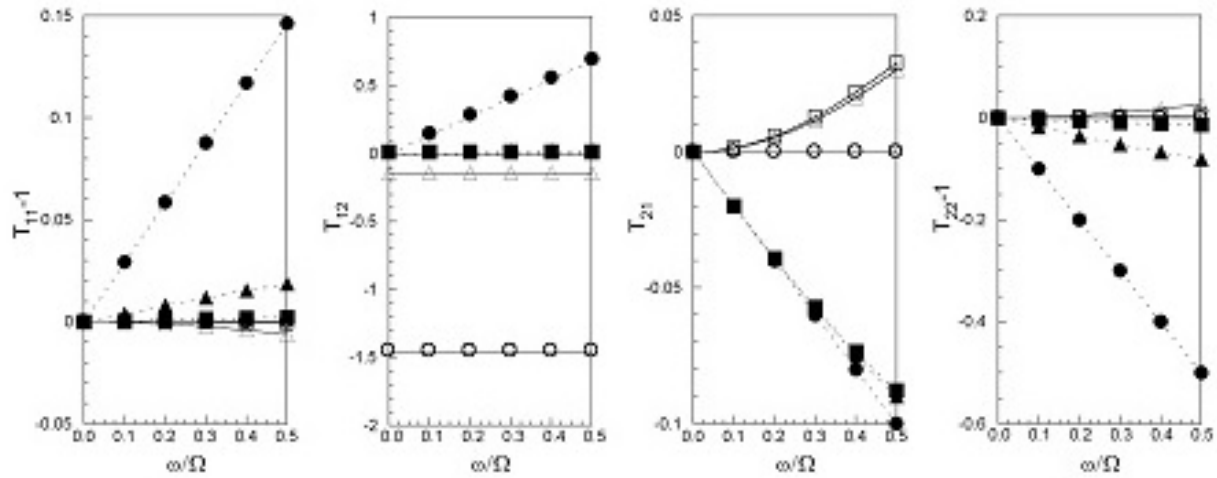


Figure 2: Calculated transfer matrices of the cavitating propeller for an advance ratio,  $J_1 = 1.0$ , and  $(K^*/2\pi, M^*) = (0.1, 1.0)$  and for various values of  $A^*/A_p = 1$  ( $\circ$ ),  $2$  ( $\triangle$ ), and  $10$  ( $\square$ ), where open and closed symbols denote the real and imaginary parts of the matrix elements respectively. From Watanabe *et al.* (2003).

exit flow angle  $\beta$  is neglected for simplicity. Note that  $T_{21}$  takes a similar value for all three cases while there are large differences in the other elements of transfer matrix.

To proceed further, appropriate values for the cavitation compliance and mass flow gain factor for a cavitating propeller must be selected and applied. As described in Section (Mfi), estimated values of  $K^*/2\pi$  and  $M^*$  for a cavitating propeller have been obtained by Otsuka *et al.* (1996) and Watanabe *et al.* (1998). They examined the unsteady planar flow through a cavitating cascade using free streamline methods (see Section (Nui)) and evaluated the cavity size per blade as a cross-sectional area  $V_{cpb}$  (not a volume). This was then applied to the three-dimensional propeller flow using the crude estimate  $V_c = Z_R R V_{cpb} / 2$ . It transpires that the resulting values of  $K^*/2\pi$  and  $M^*$  are primarily functions of the parameter  $\lambda = \sigma^*/2\alpha$ , where  $\sigma^*$  is the cavitation number *at inlet to the propeller*. Those values of  $K^*/2\pi$  and  $M^*$  are shown in Figure 3 for a propeller with typical values for the solidity ( $1.0$ ), stagger angle ( $\beta = 25^\circ$ ) and number of blades ( $Z_R = 5$ ).

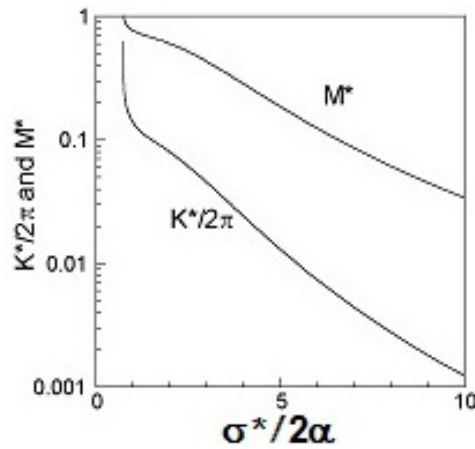


Figure 3: The estimated quasi-static cavitation compliance,  $K^*/2\pi$ , and mass flow gain factor,  $M^*$ , obtained by Watanabe *et al.* (1998) using a free streamline approach. The results plotted against  $\sigma^*/2\alpha$  are for a solidity of  $= 1.0$ , a stagger angle  $\beta = 25^\circ$  and number of blades,  $Z_R = 5$ . From Watanabe *et al.* (2003).

Now, rather than use the fixed values of  $K^*$  and  $M^*$  as was done for Figure 2, we calculate transfer functions using the above relations between  $(K^*/2\pi, M^*)$  and  $\lambda = \sigma^*/2\alpha$ . Results are shown in Figures 4 and 5 for  $A^*/A_p = 2$  and 10, respectively. Three cases with different upstream cavitation numbers  $\sigma = 0.15, 0.20$  and 0.5 are presented. The advance ratio  $J_1$  is 1.0, which is larger than the critical value. Note that, only for the case with  $\sigma = 0.15$ , is the parameter  $\lambda = \sigma/2\alpha$  less than unity and therefore only in this case is there head deterioration with increasing deviation angle. The cavitation compliance  $K^*/2\pi$  varies from 0.018 to 0.172 for  $A^*/A_p = 2$  and from 0.009 to 0.143 for  $A^*/A_p = 10$ . The mass flow gain factor  $M^*$  varies from 0.231 to 0.831 for  $A^*/A_p = 2$  and from 0.140 to 0.777 for  $A^*/A_p = 10$ . These values are slightly smaller for the case with  $A^*/A_p = 10$ .

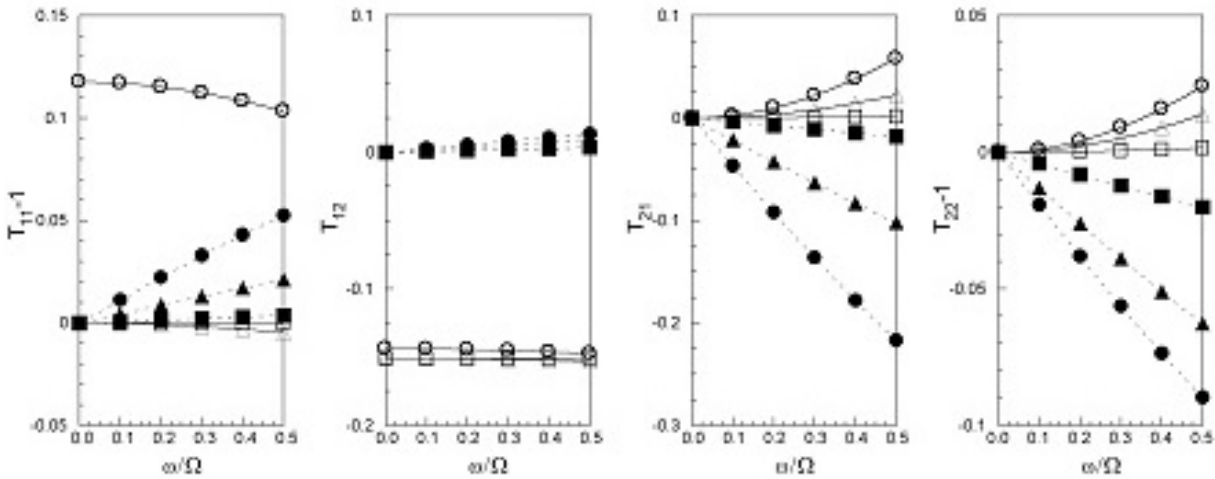


Figure 4: Calculated transfer matrices of the cavitating propeller with  $A^*/A_p = 2$  and an advance ratio,  $J_1 = 1.0$ , for the various cavitation numbers  $\sigma = 0.15$  ( $\circ$ ),  $0.20$  ( $\triangle$ ), and  $0.50$  ( $\square$ ) where open and closed symbols denote real and imaginary parts of matrix elements respectively. From Watanabe *et al.* (2003).

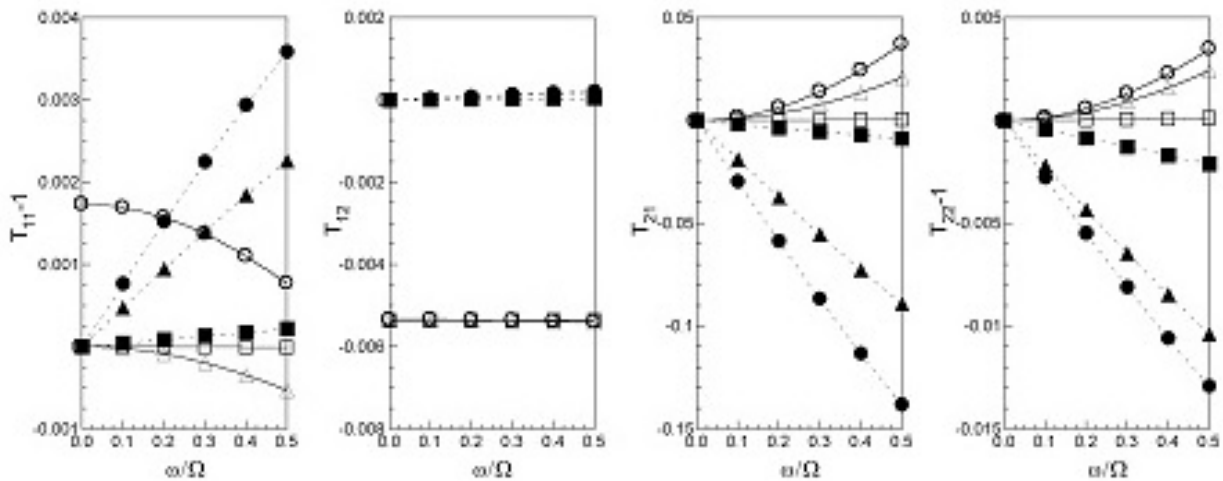


Figure 5: Calculated transfer matrices of the cavitating propeller with  $A^*/A_p = 10$  and an advance ratio,  $J_1 = 1.0$ , for the various cavitation numbers  $\sigma = 0.15$  ( $\circ$ ),  $0.20$  ( $\triangle$ ), and  $0.50$  ( $\square$ ) where open and closed symbols denote real and imaginary parts of matrix elements respectively. From Watanabe *et al.* (2003).

From Figures 4 and 5, it is seen that  $T_{21}$  takes similar values for all the cavitation numbers, while the other elements of the transfer matrix are much affected by the extent of cavitation. Note that the elements

$T_{11} - 1$ ,  $T_{12}$  and  $T_{22} - 1$  are much smaller for the case with  $A^*/A_p = 10$ , whereas the element  $T_{21}$  is the same order for both cases. This implies that the propeller with  $A^*/A_p = 10$  is more stable since the imaginary part of  $T_{22}$  is smaller; in other words the effective mass flow gain factor is smaller.

The advance ratio,  $J_1$ , is also an important parameter, because of the critical advance ratio,  $J_1^*$ , that separates normal operation from pump-like operation. It would be interesting to compare the transfer matrices for normal and pump-like operations, but unfortunately the free streamline theory is only applicable for high flow rates and high advance ratios.

The foregoing transfer functions were used by Watanabe *et al.* (2003) in investigations of the surge instability exhibited by a cavitating propeller installed in a water tunnel (Duttweiler and Brennen 1998).